Electronic and Optical Properties of Polymer Thin Films Deposited by Resonant Infrared Laser Ablation

Richard F. HAGLUND, Jr.[*], Stephen L. JOHNSON[*] and Hee K. PARK[**]

[*] *Department of Physics and Astronomy and W. M. Keck Foundation Free-Electron Laser Center*
Vanderbilt University, Nashville TN 37235-1807 U.S.A.
E-mail: richard.haglund@vanderbilt.edu

[**] *AppliFlex LLC, 320 Logue Avenue, Suite 104, Mountain View, CA 94043 U.S.A.*

Abstract. We show that polymers with electronic and electro-optic functionality can be deposited by resonant infrared pulsed laser ablation from frozen solutions and suspensions. In some cases, the addition of a co-matrix to the native solution facilitates ablation and enhances performance. As specific examples we describe the deposition of the conducting polymer PEDOT:PSS and the light-emitting polymer MEH-PPV. The conductivity of the best PEDOT:PSS films made by resonant infrared laser ablation is comparable to, and in some cases better than, that of spin-coated films. The MEH-PPV films have been incorporated into working polymer light-emitting diodes as evidence for the preservation of functionality.

DOI: 10.2961/jlmn.2007.03.0014
Keywords: Pulsed laser deposition, polymers, electronic, light-emitting, infrared laser

1. Introduction

Current liquid-phase techniques for fabricating polymer-based electro-optic, sensor and implantable biomedical devices — *e.g.*, by ink-jet deposition, spin and spray coating — face significant challenges of material deposition efficiency, solvent bleedthrough and decomposition, and lifetime degradation due to electro-chemical or biochemical activity. We have previously used resonant infrared pulsed laser deposition (RIR-PLD) to deposit many different kinds of thermoplastic and thermoset polymers [1].

We have recently deposited conductive and electroluminescent polymers by RIR-PLD, sometimes using matrix- or co-matrix-assisted ablation, and have compared the electronic properties of the RIR-PLD films with those obtained by conventional spin coating. Here we present results of these experiments on thin films of conductive and light-emitting polymers, including electrical transport measurements and spectral characterization of electro- and photoluminescence. The films prepared by RIR-PLD exhibit performance levels consistent with device requirements for electro-optic applications, such as polymer light-emitting diodes. By correlating the electronic properties of the film with the operating parameters of a picosecond, tunable free-electron laser (FEL), we can identify effects of laser fluence and wavelength on those electronic properties.

Because maintaining electronic and optical functionality, as well as preserving structural integrity, is such a stringent test of RIR-PLD, these results provide new insights into the mechanism of infrared laser ablation of intact polymers for picosecond pulses delivered at very high pulse-repetition frequencies. We will also discuss the potential for amplified, frequency-shifted ultrafast solid-state lasers, to reproduce results achieved with the FEL.

2. Materials and Experimental Procedures

Conducting polymers have many possible applications in electronics and opto-electronics [2]. Such applications include polymer thin-film transistors and polymer light-emitting diodes, charge-transport layers [3], and products and manufacturing processes that use anti-static coatings. While the technologies for polymer transistors and opto-electronic devices are not as well developed as their counterparts based on small organic molecules, the enormous versatility and range of polymer properties continues to drive interest in their development in these fields.

Polymer light-emitting diodes (PLEDs) are an emerging technology driven by the demand for low-cost flat-panel displays and new solid-state lighting applications. Made with conjugated light-emitting polymers (LEPs), PLEDs are lightweight, require relatively low power, and are intrinsically compatible with flexible displays. Since their discovery in 1990 [4], conjugated LEPs have attracted increasing interest, not least because thin LEP films can be easily deposited by liquid phase techniques such as spin coating or inkjet printing [5]. However, as improvements in device performance calls for more complex multilayered device structures, the limitations of solution phase processing become more evident. For example, solvent-polymer interaction between successive layers is difficult to avoid since the deposition of one layer could potentially dissolve or affect the layer below. Moreover, while patterning the light-emitting layer is straightforward in small molecule organic LEDs using shadow mask technology, it is more complicated for polymers dissolved in solution and requires the use of complex techniques like inkjet printing.

Since conjugated conducting and light-emitting polymers are too labile to be evaporated intact thermally, most

processing is done by liquid-phase techniques, such as spin coating or ink jet printing. However, spin coating in general is suitable for only the simplest devices, such as single-color PLEDs with one or two organic layers. Multicolor pixelated PLEDs generally require deposition of multiple layers on patterned substrate, and this is not easily done using spin coating, although it has been reported using specially synthesized light emitting polymers with photoresistive properties [6]. Ink-jet printing, while already commercially developed and currently the most common way to fabricate pixelated PLED displays, has a number of disadvantages. Since it relies on the fluidic motion of polymer solution through small nozzles, it is restricted to solutions of low viscosity [7]. Moreover, thermal ink jet printing of PEDOT:PSS on ITO can take up to ten successive depositions to create a continuous film, resulting in film thicknesses of up to 800 nm [8]. The film thickness desired for most PLEDs, on the other hand, are of order 50 nm. It is clear that while these technologies have been sufficient thus far to develop prototype devices, their large-scale implementation presents challenges that are generating interest in a more efficient and versatile deposition process.

2.1 PEDOT:PSS

One of the most widely used conducting polymers is poly(3,4-ethylenedioxy-thiophene): poly(styrenesulfonate) (PEDOT:PSS). PEDOT, the conducting component of the blend, is polymerized with the counterion PSS to yield a highly conductive (~ 10 S/cm), water-soluble polymer thin film that is nearly transparent [9]. Combined with its ability to act as a buffer layer between ITO and an organic light emitter, these qualities make it an ideal hole-transport layer in a PLED [10-12]. The structure is shown in Figure 1.

For the experiments described here, PEDOT:PSS was obtained commercially from H. C. Starck as a 1% solution in H_2O (Baytron® P). For the experiment, three different PEDOT:PSS solutions were made into frozen targets: a native PEDOT:PSS solution containing only water as the solvent, a solution containing water and a co-matrix of N-methylpyrrolidinone (NMP), and a solution containing water and a co-matrix of isopropyl alcohol (IPA).

2.2 MEH-PPV

The light emitting polymer chosen for our experiments is poly[2-methoxy-5-(2-ethylhexyloxy)-1,4-phenylene vinylene] (MEH-PPV). The chemical structure of the polymer is also shown in Figure 1. This particular polymer was chosen due to the extensive body of research that already exists. There is a previous report of IR laser transfer of MEH-PPV where a comparison was made between UV and IR laser deposition and between neat polymer and frozen matrix targets [13]. Unlike this work, however, is that here we demonstrate the deposition of MEH-PPV into a device structure (ITO/MEH-PPV/Al) to obtain devices that operate by electroluminescence, whereas in reference [13] only photoluminescence is shown.

Electroluminescent devices were fabricated both by RIR-PLD and by spin-coating for comparison purposes. For the spin-cast devices, MEH-PPV (Sigma-Aldrich, mw 40,000-70,000 amu) was dissolved as a 0.5% solution in 1,2-dichlorobenzene (DCB) and spun onto ITO coated glass. The cathode was fabricated by thermally evaporating aluminum through a shadow mask onto the polymer film, creating a device area of 0.002 cm^2 in each pixel of the shadow mask.

2.3 Laser deposition apparatus and procedure

The ablation laser used in our experiments was an rf-linac driven free-electron laser (FEL), with a wavelength that is continuously tunable from 2 to 10 μm.14 The accelerator in the FEL is powered by an S-band klystron at 2.865 GHz that produces 4 μs macropulses at a repetition rate of 30 Hz. Typical macropulse energies are of order 10-30 mJ. Within each macropulse, the small phase-space acceptance angle of the rf accelerator produces some 10^4 optical micropulses of approximately 1 ps duration. The optical bandwidth of the micropulses is typically 1% of the center frequency (FWHM) with a micropulse energy of

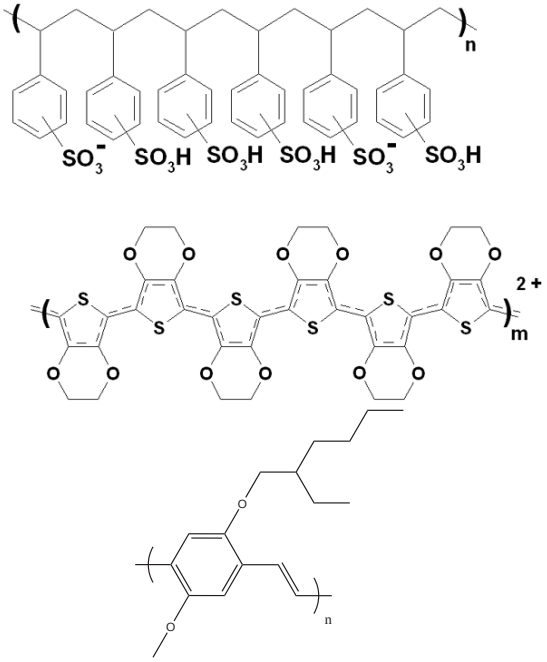

Fig. 1. Structure diagrams for the polymers discussed in this paper. From the top: PSS, the conducting polymer PEDOT and the semiconductor MEH-PPV. Full chemical nomenclature in the text.

several μJ, yielding a peak unfocused irradiance of order 10^7 W/cm^2. There we report the macropulse fluence.

The liquid solutions containing PEDOT:PSS or MEH-PPV were submerged in liquid nitrogen until frozen and the placed vertically upward inside a vacuum chamber. The FEL beam was directed through a BaF_2 window into the chamber and focused onto the target with a 500 mm focal length CaF_2 lens mounted outside the chamber. The substrate, at room temperature, was located ~3 cm above the target to collect the vaporized plume. The chamber, evacuated by a turbomolecular pumping system, had a base pressure of order 10^{-5} Torr that rose to as much as 10^{-3} Torr during ablation. The beam was rastered across the surface of the target at a linear velocity of 3 mm/s while the target was rotated at 0.5 Hz to maintain a relatively even ablation track across the surface of the frozen target. The targets typically remained frozen for up to twenty minutes.

Using a pyroelectric joulemeter, the transmission through the lens and entrance window was measured to be

approximately 0.8. Focal spot sizes were estimated from knife-edge measurements and burns on thermal paper.

3. Conductive-polymer deposition

PEDOT:PSS films were deposited on glass cover slips for scanning electron microscopy (SEM) (Hitachi S4200 SEM) and four-point probe conductivity measurements (MMR H-50 Van der Pauw System), and on NaCl disks for FTIR spectroscopic analysis (Bruker IFS 66v FTIR spectrometer). In the conductivity measurements, the accuracy of the data was limited by the inhomogeneity of the film surface and thickness variations between different samples.

For the various PEDOT:PSS solutions, the FEL was tuned to a vibrational resonance of one of the matrix components. Fourier transform infrared (FTIR) spectra of the solvents used in these experiments are shown in with the targeted vibrational modes for each solvent. Since the full width half maximum (FWHM) of the water O-H stretching resonance is sufficiently separated from the FWHM of the C-H stretching resonances of the IPA and NMP, it is possible to selectively tune the FEL to specifically excite one matrix even if two matrices are present. The linewidth of the FEL in this region is typically 50 nm so that some overlap occurs, but most of the laser energy is deposited into one specific matrix absorption mode.

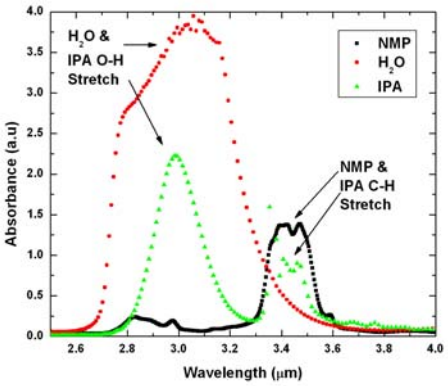

Fig. 2. FTIR spectra of PEDOT:PSS solutions when mixed with NMP and isopropyl alcohol (IPA).

3.1 NMP as a co-matrix

The process of depositing films by dispersing the desired component in a matrix at low concentration in a matrix and then ablating at a resonant absorption of the matrix is often called matrix-assisted pulsed laser evaporation (MAPLE). While both ultraviolet (UV) and resonant infrared (RIR) MAPLE have been shown to produce good results with biological molecules 15, the results in this case were initially disappointing: RIR-MAPLE of PEDOT:PSS using the resonant absorption band of water ice produced rough films that were non-conducting.

In an effort to produce electrically conductive films, N-methylpyrrolidinone (NMP), a known conductivity enhancer in spin-coated PEDOT:PSS films, was doped into the target material 16. The NMP concentration was varied between 5% and 50% by weight. As seen in Figure 2, the FWHM of the C-H stretch at 3.47 μm is well isolated from the O-H stretch of water at 3.05 μm. When the either the H_2O or the NMP matrix is excited, films are conductive and exhibited an improved morphology when compared to films deposited without a co-matrix. The FTIR spectra of the films also compared very well to a spectrum taken of a spin coated film. However, it should be noted that little if any difference between conductive and non-conductive films was evident in the FTIR spectra; evidently the FTIR signature indicates only that .

Conductivities of PEDOT:PSS films deposited from targets prepared with different concentrations of NMP are displayed in Table I. Note that when water is used as the excitation matrix, the film conductivities are dependent on NMP concentration, but independent of it when the NMP matrix is excited.

Table 1 Conductivities of PEDOT:PSS films

% NMP	Wavelength (μm)	Conductivity (W·cm)
0	Spin-coating	14.7±2.9
0	3.05	0
10	3.05	39.5±22
50	3.05	11.7±8.9
10	3.47	5.65±0.5
50	3.47	5.2±1.7

3.2 IPA as a co-matrix

To further investigate the role of a co-matrix, isopropyl alcohol (IPA), also described by its manufacturer as a conductivity enhancer for PEDOT:PSS, was doped into the PEDOT:PSS solution prior to freezing. As seen from Figure 2, target irradiation at 3.05 μm deposits energy into both the water and the IPA matrices since both contain an O-H bond, but 3.36 – 3.47 μm irradiation excites only the C-H bond in the IPA co-matrix. Since the O-H resonance in IPA has a lower cross section than that of H_2O, more of the photon energy at 3.05 μm is absorbed by the water matrix, but the absorbed laser light is shared between the two vibrational modes.

While the films deposited with the IPA co-matrix are not quite as smooth as those deposited with NMP, they are still superior to films deposited from unmixed PEDOT:PSS targets. The most interesting result of the four-point probe measurements on films deposited with IPA as a co-matrix is that films deposited using 3.05 μm irradiation (O-H stretch of water ice and IPA) are not conductive, whereas those deposited using 3.36 μm irradiation (the C-H stretch mode of the IPA) are. The PEDOT:PSS films deposited with an IPA co-matrix (not shown) are conductive at 3.36 μm, but not at 3.05 μm. This suggests that the role of the co-matrix is very complex, certainly more differentiated than the use of the matrix as a simple light absorber and carrier for the PEDOT:PSS that is typical of IR-MAPLE.

4. Deposition of electro-/photoluminescent polymers

Deposition of MEH-PPV was rather more complicated than for the PEDOT:PSS, because the MEH-PPV powder is not easily soluble, even in DCB. The absorption spectrum of DCB is shown in Figure 3. For RIR-PLD, the FEL was tuned to either the C-H stretch of the DCB at 3.26 µm, or the C=C-C ring mode at 6.86 µm.

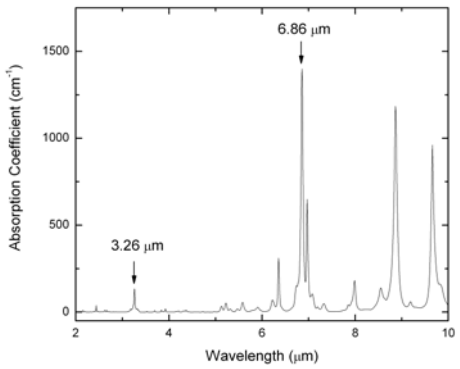

Fig. 3. FTIR spectrum of dichlorobenzene. The arrows indicate the wavelengths to which the FEL was tuned to initiate ablation of the frozen MEH-PPV solution.

4.1 Deposition morphology for MEH-PPV

FTIR spectroscopy (Bruker IFS 66v FTIR spectrometer) was employed to analyze the bonding structure of the MEH-PPV after deposition. The similarity between the spin coated spectrum and the spectra of laser deposited MEH-PPV reveals that the local structure of the polymer is preserved throughout the laser deposition. It was also found that there was essentially no differences between the

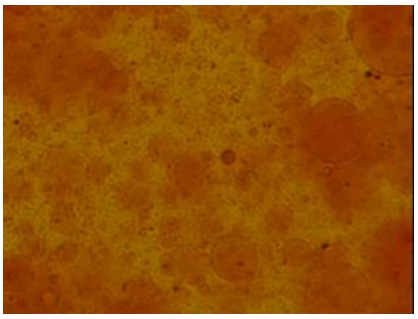

Fig. 4. Droplet formation in a typical MEH-PPV deposition. The MEH-PPV was suspended in dichlorobenzene, frozen and then ablated. The droplets are smaller and denser for smaller focal spots, and also for more viscous solvents.

spectra of MEH-PPV deposited by laser ablation at different fluences. The fact that the spectra are independent of the laser fluence (at least up to ~ 5 times above threshold) suggests that the matrix probably absorbs most of the laser energy and shields the polymer from interaction with the energetic matrix debris, allowing it to be deposited intact.

An optical micrograph of a typical laser-deposited MEH-PPV film is shown in Figure 4. The surface layer in all cases exhibits a large density of droplets, with some variation depending on laser fluence and solvent viscosity. The existence of the droplets can likely be explained in one of two ways. One possibility is that the target surface melts after some exposure to the laser, but before the end of the full macropulse; the remainder of the macropulse impinging on the liquid surface causes "splashing" of the liquid target onto the substrate. Another possibility is that the laser directly ejects "chunks" of the frozen polymer solution that stick to the substrate and then melts. Both of these scenarios are plausible; at this point it is unclear which is in fact responsible for the abundance of droplets. The size and density of the droplets vary with laser fluence and solvent viscosity; also it is found that ablation of the MEH-PPV target at the 6.86 µm band generates fewer droplets than at 3.26 µm.

4.2 Electronic response of the MEH-PPV films

To investigate the electrical behavior of the PLED devices, I-V curves were measured and are displayed in Figure 5. It is immediately noticeable that the "turn-on voltage" of the FEL devices is much lower than that of the spin coated device. This can partly be explained by the difference in film thickness between the laser deposited devices and the spin coated device. The laser deposited films appeared by the eye to be slightly thinner than the spin coated devices, which would explain their lower turn-on voltage. Measurements with a stylus profilometer showed a very rough film, with an average thickness of order 35±30 nm. It is doubtful, however, that the thicknesses of the various films differ by the same factor of ~ 3 observed in the threshold voltage values.

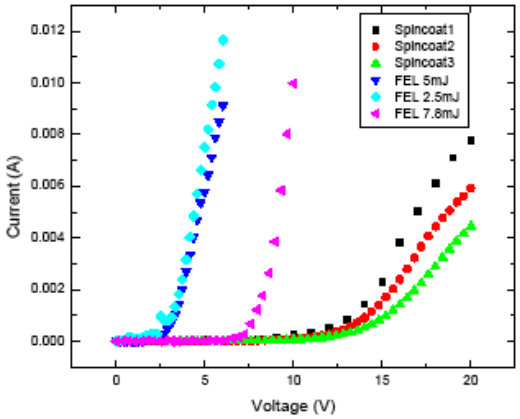

Fig. 5. I-V curves for MEH-PPV films deposited by spin coating and by the free-electron laser at various FEL macropulse energies as shown.

The slopes of the *I-V* curves for the laser deposited devices are also steeper than that of the spin-coated devices. In addition, it appears that there is, in addition, a fluence dependence that suggests the possible of laser-induced alteration of the MEH-PPV at high fluences. However, the fluence dependence may also simply be indicative of a thicker film and therefore a higher turn-on voltage. Whether or not the differences in the slope of the *I-V* curves is also a result of some laser-induced process is unknown at this point and is currently under investigation. A quantitative study of film thickness *vs* conductivity is important to correctly interpret these data, and such measurements are underway.

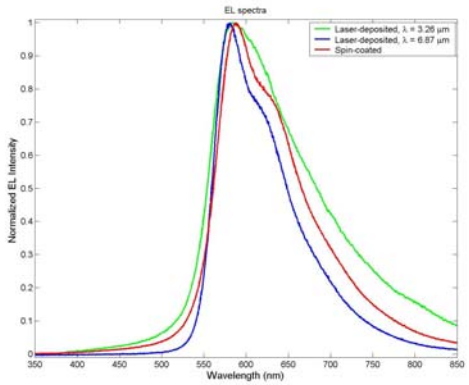

Fig. 6. Electroluminescence spectra for the MEH-PPV light-emitting diodes made by spin coating (purple trace) and by FEL deposition at the indicated wavelengths. Macropulse fluence was of order 3J/cm^2.

4.3 Electroluminescence spectra of MEH-PPV

Electroluminescence (EL) spectra were acquired for both spin-coated and laser-fabricated devices and are shown in Figure 6. While there is no significant shift in the peak emission wavelength of the FEL created devices with respect to the spin coated device, there is some modest spectral broadening that seems to increase with increasing laser fluence, The fact that the peak emission wavelength is not shifted for the laser-deposited devices attests the intact deposition of MEH-PPV chains. It is well known that decreasing the conjugation length of the polymer leads to an increase in bandgap and a resulting blue-shift in emission wavelength. The broadening of the peaks could come from a slight change in conjugation length induced by the laser ablation event, but with the average conjugation length remaining roughly the same. This could be a result of some fragmented species caused by the ablation event and the combination of some of these fragments with intact chains to form species of longer conjugation lengths. This would explain the spectral broadening while the peak emission wavelength remains constant. Some form of mass spectrometry like gel permeation chromatography (GPC) or matrix-assisted laser desorption and ionization time of flight (MALDI-TOF) mass spectrometry could more firmly address this issue and these experiments will likely be done in the future.

5. Solid-state lasers for infrared laser ablation

The results achieved using the free-electron laser are interesting from the standpoint of thin-film deposition research, but an FEL is far too expensive and complex to be used in the commercial production of micro- and nanostructured organic and polymeric films. Nevertheless, the experimental results achieved thus far point the way toward the development of laser systems more suited to commercial and industrial applications.

Why is the unique macropulse-micropulse time structure of the free-electron laser so well suited to the ablation of intact polymers? The FEL irradiation has several critical properties that all seem necessary to provide efficient, but still gentle, ablation: (1) The O-H and C-H vibrational resonances are localized excitation modes of the monomer units of the polymer in question. (2) A micropulse delivering 1 μJ to one of these resonant excitations conveys of order one photon per nm^3 — a significant vibrational excitation density. (3) The picosecond micropulse has a duration shorter than the stress confinement time, given by

$$\tau_{micro} << \tau_{stress} \approx \frac{L_{opt}}{C_s} \sim 0.01 - 0.1 \ \mu s \qquad (1)$$

where L_{opt} is the optical penetration depth and C_s is the speed of sound. This means that each micropulse delivers its quantum of energy in a time scale short compared to typical stress relaxation times — and that the absorbed laser energy will be fully equilibrated before the arrival of the next micropulse. (4) The FEL macropulse can be adjusted so that it has a duration less than the thermal confinement time, given by

$$\tau_{macro} << \tau_{thermal} \approx \frac{L_{opt}^2}{\kappa} \sim 0.1 - 1 \ \mu s \qquad (2)$$

where κ is the thermal diffusivity. This ensures that the total energy deposited goes into the absorption volume and does not diffuse into the cold surrounding material to create a heat-affected zone that "cooks" the polymers.

Thus the issue of replacing the FEL revolves around the question of whether or not it is possible to generate such a pulse structure in a solid-state laser, and to provide at least

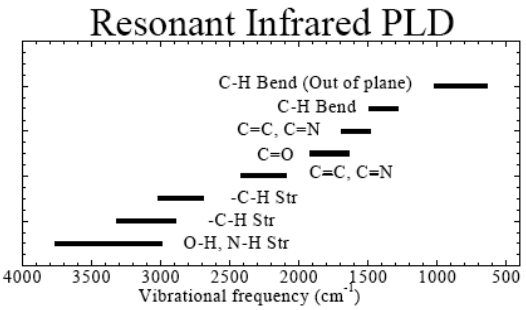

Fig. 7. Vibrational modes of potential interest for polymer and nanoparticle coatings. The C-F modes of fluorinated polymers are not shown; these bands lie in the 1200 cm^{-1} range.

sufficient tunability to deposit energy in the wavelength ranges relevant to polymers. Most of these bands are shown in Figure 7. The most important ones for the applications discussed here are the O-H, C-H and N-H stretching vibrations. However, excitation of bands in the 6-7 μm region produce efficient deposition of both MEH-PPV and the small light-emitting molecule Alq_3. Moreover, one of the most interesting potential polymers — the insoluble polytetrafluoroethylene (trade name, Teflon®) — can be deposited by exciting the C-F_2 stretching mode at 8.26 μm [17]. The challenge is how to reach these wavelengths using presently available nonlinear infrared materials.

Recent publications [18-20] suggest that the combination of a high repetition-rate pump laser such as Nd:YAG or Yb:YAG coupled to an optical parametric oscillator (OPO) [21] may well be capable of producing a high-repetition rate pulse structure with significant average power in the mid-infrared range. However, it will clearly

be a challenge to develop the macropulse-micropulse structure that appears to be so effective with the FEL. Moreover, the development of mid-infrared materials to cover the wavelength bands of interest (see Figure 7) and to find suitable sources of radiation to provide the idler beam for the OPO seems particularly difficult at this time. The only way at present to achieve wavelengths beyond 4 μm is at present to cascade successive OPO stages, with the attendant cost in efficiency at each stage. It may well be that the development of mode-locked Cr-doped ZnSe lasers, as well as the development of advanced IR frequency-conversion materials (*e.g.*, glass-bonded GaAs laminates) will move us forward toward ablation of polymers with interesting bands in the 6-9 μm region of the spectrum.

6. Relevance to laser precision microfabrication

Resonant infrared pulsed laser deposition has potential for significant impact on microfabrication, because it represents one of the few ways in which thin films of functionalized polymers or nanoparticles with desirable chemical and electronic properties can be easily incorporated into MEMS and NEMS structures. RIR-PLD, because it is a vacuum deposition process, is by its nature adaptable to all of the conventional techniques that have been used to produce inorganic and small-molecule organic coatings in other thin film applications. Because RIR-PLD, like other laser ablation processes, is strongly forward directed, it is inherently less wasteful of the starting film materials than evaporative processes. This is particularly significant for high-value polymers — such as electronically or electro-optically active materials — which can cost many hundreds of dollars per gram. Moreover, the versatility of the method in terms of materials — so far, every polymer that has been tried with RIR-PLD has been deposited intact as long as one stays below the entanglement limit — adds an enormous range of useful coatings to the designer of OLED, PLED, MEMS, NEMS or other micro-fabricated devices. Last, but surely not least, the fact that polymer films can be deposited with good adhesion and other properties on inorganic substrates creates many new opportunities for designing organic-inorganic interfaces.

Acknowledgments

The authors thank the staff of the W.M. Keck Foundation Free-Electron Laser Center for their skillful operation of the laser source. We also thank K. E. Schriver for insightful discussions and to E. U. Donev and J. Rozen for help in data acquisition. S. L. Johnson thanks AppliFlex LLC for financial support. The operation of the Free-Electron Laser Center is supported by the Medical FEL Program of the Department of Defense administered by the Air Force Office of Scientific Research (Contract F49620-01-1-0429).

7. References

[1] For a review, see D. M. Bubb and R. F. Haglund, Jr.: "Resonant Infrared Pulsed Laser Ablation and Deposition of Thin Polymer Films," ed. by R. Eason, (John Wiley and Sons, New York, 2006),p. 35.

[2] A. J. Heeger, Reviews of Modern Physics **73**, 681 (2001).

[3] G. Malliaras and R. Friend, Physics Today **58**, 53 (2005).

[4] J. H. Burroughes, D. D. C. Bradley, A. R. Brown, R. N. Marks, K. Mackay, R. H. Friend, P. L. Burns and A. B. Holmes, Nature **347**, 539 (1990).

[5] R. H. Friend, R. W. Gymer, A. B. Holmes, J. H. Burroughes, R. N. Marks, C. Taliani, D. D. C. Bradley, D. A. Dos Santos, J. L. Bredas, M. Logdlund and W. R. Salaneck, Nature **397**, 121 (1999).

[6] C. D. Muller, A. Falcou, N. Reckefuss, M. Rojahn, V. Wiederhirn, P. Rudati, H. Frohne, O. Nuyken, H. Becker and K. Meerholz, Nature **421**, 829 (2003).

[7] B. J. de Gans, P. C. Duineveld and U. S. Schubert, Advanced Materials **16**, 203 (2004).

[8] B. Ballarin, A. Fraleoni-Morgera, D. Frascaro, S. Marazzita, C. Piana and L. Setti, Synthetic Metals **146**, 201 (2004).

[9] B. L. Groenendaal, F. Jonas, D. Freitag, H. Pielartzik and J. R. Reynolds, Advanced Materials **12**, 481 (2000).

[10] M. P. de Jong, L. J. van IJzendoorn and M. J. A. de Voigt, Applied Physics Letters **77**, 2255 (2000).

[11] S. A. Carter, M. Angelopoulos, S. Karg, P. J. Brock and J. C. Scott, Applied Physics Letters **70**, 2067 (1997).

[12] A. Berntsen, Y. Croonen, C. Liedenbaum, H. Schoo, R. J. Visser, J. Vleggaar and P. van de Weijer, Optical Materials **9**, 125 (1998).

[13] B. Toftmann, M. R. Papantonakis, R. C. Y. Auyeung, W. Kim, S. M. O'Malley, D. M. Bubb, J. S. Horwitz, J. Schou, P. M. Johansen and R. E. Haglund, Thin Solid Films **453-54**, 177 (2004).

[14] G. S. Edwards, D. Evertson, W. Gabella, R. Grant, T. L. King, J. Kozub, M. Mendenhall, J. Shen, R. Shores, S. Storms and R. H. Traeger, Ieee Journal Of Selected Topics In Quantum Electronics **2**, 810 (1996).

[15] D. B. Chrisey, A. Pique, R. A. McGill, J. S. Horwitz, B. R. Ringeisen, D. M. Bubb and P. K. Wu, Chemical Reviews **103**, 553 (2003).

[16] F. Louwet, L. Groenendaal, J. Dhaen, J. Manca, J. Van Luppen, E. Verdonck and L. Leenders, Synthetic Metals **135**, 115 (2003).

[17] M. R. Papantonakis and R. F. Haglund, Applied Physics a-Materials Science & Processing **79**, 1687 (2004).

[18] E. Innerhofer, T. Sudmeyer, F. Brunner, R. Haring, A. Aschwanden, R. Paschotta, C. Honninger, M. Kumkar and U. Keller, Optics Letters **28**, 367 (2003).

[19] U. Keller, Nature **424**, 831 (2003).

[20] F. Brunner, E. Innerhofer, S. V. Marchese, T. Sudmeyer, R. Paschotta, T. Usami, H. Ito, S. Kurimura, K. Kitamura, G. Arisholm and U. Keller, Optics Letters **29**, 1921 (2004).

[21] E. Innerhofer, T. Sudmeyer, F. Brunner, R. Paschotta and U. Keller, Laser Physics Letters **1**, 82 (2004).

(Received: May 8, 2007, Accepted: October 18, 2007)